Photophysics of Some Disubstituted Indoles and Their Involvements in Photoinduced Electron Transfer Reactions

S. K. Pal,[†] T. Bhattacharya,[†] T. Misra,[†] R. D. Saini,[‡] and T. Ganguly*,[†]

Department of Spectroscopy, Indian Association for the Cultivation of Science, Jadavpur, Kolkata 700 032, India, and Radiation Chemistry and Chemical Dynamics Division, Bhabha Atomic Research Center, Mumbai 400 085, India

Received: September 24, 2003

Steady state electronic absorption, fluorescence emission, polarized spectra of some disubstituted indoles, 2,3-dimethylindole (23DMI), 2,5-dimethylindole (25DMI), and 1,2-dimethylindole (12DMI), were studied in solvents of different polarity coupled with time resolved measurements. The electrochemical measurements demonstrate that DMIs should act as electron donors in photoinduced electron transfer (PET) reactions with 9Cyanoanthracene (9CNA) which serves as the electron acceptor. The photoexcited 9CNA undergoes fluorescence quenching in the presence of DMI both in nonpolar *n*-heptane (NH) and highly polar acetonitrile (ACN) solvents though no ground state complex formation was apparent between the reactants. In NH, the observation of the reduction of fluorescence emission intensity of 9CNA accompanied by the formation of emissive exciplex was made only for the *N*-methyl substituted indole 12DMI. Transient absorption spectra recorded by the laser flash photolysis technique show that photoinduced charge separation reaction proceeds both in the excited singlet and triplet states of 9CNA. Moreover, it is also established that production of the monomeric triplet of 9CNA occurs through the ion recombination mechanism. In NH, the possibility of the formation of a contact neutral radical, through the H-atom transfer reaction, as an additional route for rapid nonradiative decay of the exciplex is hinted at in the case of N−H indoles 23DMI and 25DMI. Nevertheless, it is inferred that in the case of 12DMI the observed emissive exciplex in nonpolar medium is due to its inability to form a contact neutral radical. In ACN, the major nonradiative pathway appears to be due to photoinduced ET rather than formation of exciplex.

1. Introduction

To develop a basic understanding of redox proteins,[1−4] investigations on the photophysics and photochemistry of indoles still remain a very important subject of active research. These studies are also helpful in revealing the mechanism of long-range electron transfer in proteins as indole is a chromophore of the amino acid tryptophan. Mackintosh and his groups[5,6] and Jennings et al.[7] showed that the electrochemically generated monosubstituted indole polymer films exhibit intense visible photoluminescence and therefore they are potential candidates for the development of new electroluminescent materials. Thus, the interest in the newly developed artificial photosynthetic devices (dyad or triad system) with indole or substituted indoles as donors not only is concerned with their properties as photoconducting materials but attention should also be given to their luminescence properties. As most of the photophysical work was done on the monosubstituted indoles, we were interested to see the photophysics of disubstituted ones. Nevertheless, in the present work, we have focused our attention on the charge transfer or electron transfer (ET) reactions within the present disubstituted indoles (DMIs) (Figure 1): 1,2-dimethylindole (12DMI), 2,3-dimethylindole (23DMI), and 2,5-dimethylindole (25DMI) and the well-known electron acceptor

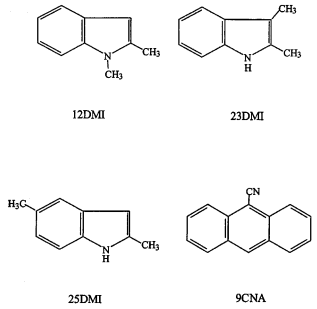

Figure 1. Molecular structures of 12DMI, 23DMI, 25DMI, and 9CNA.

9Cyanoanthracene (9CNA). We already reported[8] the photophysical and electron donating properties of several (monosubstituted) methylindoles. From the values of the half-wave oxidation potentials of the disubstituted indoles, measured by electrochemical technique (vide infra), it indicates that electron donating capabilities of the present disubstituted indoles are larger than those of the monosubstituted indoles derivatives. It is hoped that much potential artificial photosynthetic materials could be developed with these disubstituted indoles and 9CNA, being connected together by rigid /flexible spacers. Before synthesizing such artificial devices, systematic studies were made by both steady state and time-resolved spectroscopic techniques to reveal the mechanism of bimolecular photoinduced electron-transfer reactions in solution between the redox sites DMIs and 9CNA. It is expected that these intermolecular investigations could be helpful to gain better insights into the

* To whom correspondence should be addressed. E-mail: sptg@mahendra.iacs.res.in. Phone: +91 33 2473 4971/3073 × 266. Fax: +91 33 2473 2805.
[†] Indian Association for the Cultivation of Science.
[‡] Bhabha Atomic Research Center.

10.1021/jp0311005 CCC: $25.00
Published on Web 11/11/2003

mechanism of ET within the bichromophoric or multichromophoric systems comprising both DMI as donor and 9CNA as acceptor. In the present paper, the results and their interpretations have been presented.

2. Experimental Section

2.1. Materials. All of the samples 12DMI, 23DMI, 25DMI, and 9CNA (97% pure), supplied by Aldrich, were purified by vacuum sublimation. The solvents *n*-heptane (NH), acetonitrile (ACN) (SRL), and ethanol (EtOH) of spectroscopic grade were distilled under vacuum according to the standard procedure and tested before use for the presence of any impurity emission in the wavelength region studied.

2.2. Spectroscopic Apparatus. At the ambient temperature (296 K), steady-state electronic absorption and fluorescence emission spectra of dilute solutions ($10^{-4}-10^{-6}$ mol dm^{-3}) of the samples were recorded using a 1 cm path length rectangular quartz cells by means of an absorption spectrophotometer (Shimadzu UV−VIS 2101PC) and F-4500 fluorescence spectrophotometer (Hitachi), respectively. Fluorescence lifetimes were measured by using a time-correlated single photon counting (TCSPC) fluorimeter constructed from components purchased from Edinburgh Analytical Instruments (EAI), model 199 UK. The experimental details are given elsewhere.[9] The goodness of fit has been assessed with the help of statistical parameters χ^2 and DW. All of the solutions prepared for room-temperature measurements were deoxygenated by purging with an argon gas stream for about 30 min.

The degree of polarization (P) was measured with the help of UV−VIS polarizer accessories including UV Linear Dichroic polarizer, wavelength range 230−770 nm, purchased from Oriel Instruments, U.S.A. The observed degree of polarization (P) values were obtained from the following relation:[10]

$$P = [I_{EE} - (I_{BE}/I_{BB})I_{EB}]/[I_{EE} + (I_{BE}/I_{BB})I_{EB}] \qquad (1)$$

Here, I_{EE} and I_{EB} are the intensities of parallel and perpendicular polarized emission with vertically polarized excitation and I_{BB} and I_{BE} are the intensities of horizontally and vertically polarized emission when excited with horizontally polarized light. I_{BE}/I_{BB} defines the instrumental correction factor G (polarization characteristic of the photometric system). This correction is made for any change in the sensitivity of the emission channel for the vertically and horizontally polarized components.

2.3. Laser Flash Photolysis. The third harmonic (355 nm) output pulses of 35 ps duration and energy ~6 mJ pulse^{-1} from an active-passive mode-locked Nd:YAG laser (Continuum, model 501-C-10) were used for excitation of the samples. Transients were studied by monitoring their absorption using a tungsten filament lamp in combination with a Bausch and Lomb monochromator (f/10, 350−800 nm), Hamamatsu R 928 PMT, and a 500 MHz digital storage oscilloscope (Tektronix, TDS-540A) connected to a PC.

2.4. Electrochemical Measurements. Electrochemical measurements to determine the redox potentials of the reactants were made by using the PAR model 370-4 electrochemistry system. Three electrode systems including SCE as a standard were used in the measurements. Tetraethylammonium perchlorate (TEAP) in ACN was used as the supporting electrolyte as before.[11]

3. Results and Discussion

3.1. Studies on Spectroscopic Properties. *3.1.1 Steady-State Electronic Absorption Spectra at Ambient Temperature.* From the electronic absorption spectra of DMIs in various solvents (Figure 2), it was observed that all three compounds exhibit absorption band system in the region of 215−325 nm. The absorption bands of these compounds look very similar to the corresponding bands of methylindoles,[8] and the lower energy electronic absorption band envelopes of DMIs, residing within 260−325 nm, should be due to overlapping of two closely lying electronic transitions $^1L_b \leftarrow {}^1A$ and $^1L_a \leftarrow {}^1A$. When the polarity of the medium is increased from NH to EtOH to ACN, the (0,0) band position (~291 nm) remains unaltered but the absorption maximum (~281 nm) undergoes a small red shift. Following the assignments made by Meech et al.,[12] it may be argued that the (0,0) band being unperturbed by the polarity of the solvent may be due to $^1L_b \leftarrow {}^1A$ transition, and the band maximum could be assigned to $^1L_a \leftarrow {}^1A$ transition. The band at the much higher energy region, around the 225 nm position, is probably due to the transition $^1B_b \leftarrow {}^1A$.[13] However, to assign the nature of the absorption bands unambiguously, steady-state polarization measurements were carried out which has been discussed below.

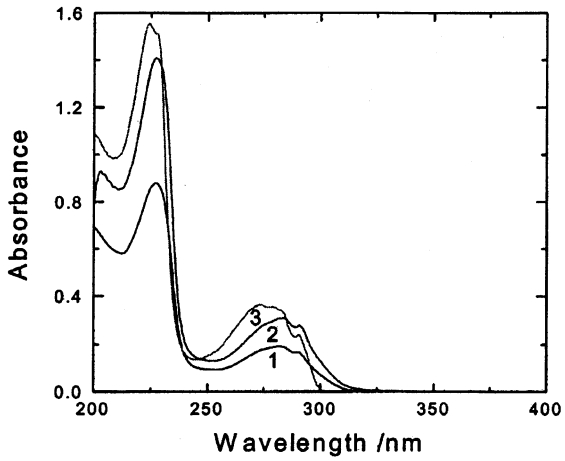

Figure 2. Steady-state electronic absorption spectra of 23DMI in (1) ACN, (2) and EtOH, (3) NH.

3.1.2. Polarized Fluorescence Excitation Spectra. In nonpolar NH, the fluorescence emissions of the DMIs, produced by exciting at either 281 or 291 nm, exhibit maxima at the same energy positions. However the emission undergoes significant red shift with change of the polarity of the surrounding solvent, e.g., from NH to highly polar ACN (or polar protic solvent EtOH).

In the present investigation, the polarized fluorescence excitation spectra (Figure 3) were measured for the DMIs in polar EtOH rigid glassy matrix at 77 K to avoid the Brownian rotational depolarization[14,15] effect. While measuring the degree of polarization (P), the necessary corrections were made for the instrumental factor.[16]

From Figure 3, it is found that the fluorescence excitation polarization spectra, measured by monitoring at the fluorescence maximum 350 nm, exhibit a positive P value (~0.23) at the absorption band maximum around 281 nm and a relatively high positive P value (~0.28) at the (0,0) band position around 291 nm. This observation demonstrates that in the case of the absorption spectra of a DMI the nature of the band maximum differs from that of the (0,0) band. The band around 2910 Å has been assigned to mostly ^1L_b and the band at 2810 Å to ^1L_a. These assignments were made on the understanding that the fluorescence emission of the compound should originate primarily from the lower ^1L_b state. Because the theoretical plateau for P is +0.5 and −0.33, the P values observed in the present investigation indicate that some mixed state of ^1L_a and ^1L_b is responsible for the observed low energy absorption band

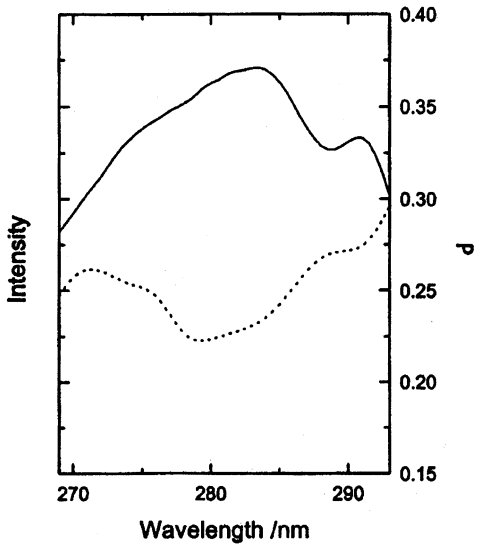

Figure 3. Solid line represents the fluorescence excitation spectra of 23DMI in EtOH rigid glassy matrix at 77 K, and the broken line shows the excitation polarization spectra.

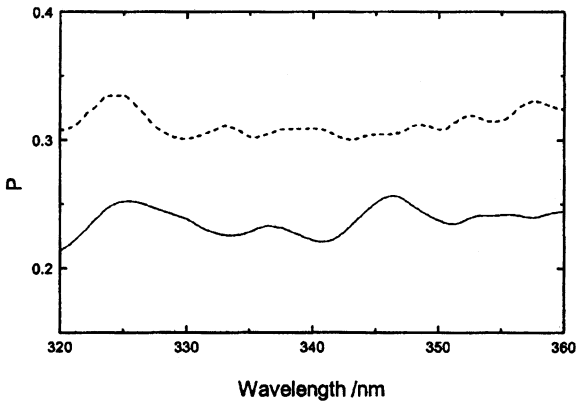

Figure 4. Fluorescence polarization spectra of 23DMI in EtOH rigid glassy matrix at 77 K with excitation wavelength at (1) 291 nm (broken line) and (2) 281 nm (solid line).

spanning between 260 and 325 nm though the contribution of ^1L_b state appears to be much prominent (P∼+0.28) at the (0,0) band position. Fluorescence polarization studies (Figure 4) also reveal that the fluorescence is primarily originating from the ^1L_b state but the contribution of the ^1L_a state in emission could not be ignored as the *P* values obtained (∼+0.3), due to excitation with 295 *nm* (region of mostly ^1L_b), were less than the maximum possible value (+0.5) for the pure state. When excitation was made at 281 nm, a domain of primarily ^1L_a, expectedly, the magnitudes of positive values of *P* decrease (Figure 4).

3.2. Possibility of Photoinduced Electron Transfer (PET) within the Present Donor Acceptor Systems. *3.2.1. Electrochemical Studies.* The half-wave oxidation potentials ($E_{1/2}^{OX}(D/D^+)$) of 12DMI, 23DMI, and 25DMI and the half-wave reduction potential ($E_{1/2}^{RED}(A^-/A)$) of 9CNA were measured by using cyclic voltammetry (details were given in the Experimental Section), and the values are shown in the Table 1. The observed values indicate that the present DMIs act as electron donors (D) in the presence of 9CNA which in turn serves as an electron accepting species (A) in the PET reaction. The possibility of occurrence of PET within the present donor acceptor systems has been predicted by computing the Gibb's free energy of ET reactions (ΔG_{ET}^0) from the well-known Rehm−Weller relation[17−19]

TABLE 1: Redox Potentials of the Reactive Sites and Gibbs Free Energies (ΔG°) Associated with Photoinduced ET Reactions in ACN Fluid Solutions at 296 K

D−A system[a]	$E_{1/2}^{OX}$ (D/D^+)/V	$E_{1/2}^{RED}$ (A^-/A)/V	$E_{0,0}^*$/eV	ΔG_{ET}^0/eV
23DMI+9CNA[a]	+0.898	−1.13	3.08	−0.99
12DMI+9CNA[a]	+0.678	−1.13	3.08	−1.33
25DMI+9CNA[a]	+0.632	−1.13	3.08	−1.38
23DMI+9CNA	+0.898	−1.13		+2.03
12DMI+9CNA	+0.678	−1.13		+1.81
25DMI+9CNA	+0.632	−1.13		+1.76

[a] Denotes the first excited singlet state (S_1). $E_{0,0}^*$ is the singlet−singlet 0,0 transition energy of the excited chromophore.

$$\Delta G_{ET}^0 = E_{1/2}^{OX}(D/D^+) - E_{1/2}^{RED}(A^-/A) - E_{0,0}^* - e^2/4\pi\epsilon_0\epsilon_s R \quad (2)$$

$E_{0,0}^*$ is the first singlet−singlet transition energy ((0,0) band) of the acceptor and fourth term represents the coulomb stabilization term whose contribution to the value of ΔG_{ET}^0 is negligible (∼0.06 eV) in highly polar solvent ACN. ΔG_{ET}^0 values for different donor−acceptor systems in ACN are listed in Table 1. From the table, it is apparent that from the thermodynamic point of view the photoinduced ET process is primarily responsible for the quenching mechanism (discussed below) and the occurrence of ET reactions should be in the intermediate region (0.4 eV < $-\Delta G_{ET}^0$ < 2.0 eV).[20]

3.2.2. Spectroscopic Investigation. Bimolecular quenching rate constants, k_q, were determined in NH, EtOH, and ACN solvents from linear Stern−Volmer (SV) plots obtained from the reductions of the fluorescence intensity (Figure 5a−c) and the fluorescence lifetime (τ_0) of 9CNA was determined as function of quencher (DMI) concentrations. As the fluorescence quenching of 9CNA occurs in the region of DMI concentrations where the absorption spectrum of 9CNA is not at all affected, the simple SV equation was used to analyze the observed quenching. The values of k_q measured from SV plots obtained from steady state and time resolved spectroscopic studies (Figure 6) are found to be the same within the experimental error and nearly equal to k_d, the diffusion-controlled rate (Table 2). This indicates the involvement of dynamic process in quenching mechanism. At the excitation wavelength (∼402 nm for 9CNA), quencher molecules (donors) are transparent. Moreover, no ground-state complex formation was apparent from the measurements of the electronic absorption spectra of the mixtures of the present quencher and fluorescer molecules, having the similar concentrations as used in the above quenching studies. At ambient temperature, the absorption spectra of the mixture of the donor (23DMI or 12DMI or 25DMI) and the acceptor 9CNA appear to be just a superposition of the corresponding spectra of the individual reactants irrespective of the polarity of the surrounding solvents (Figure 7). This observation rules out the possibilities for the presence of any static quenching mode in the observed quenching phenomena of 9CNA.

In highly polar ACN solution, the fluorescence of 9CNA is sufficiently quenched by DMIs over the entire band envelope (Figure 5a). The estimated bimolecular rate constants are found to be nearly equal to the diffusion controlled limit in the case of all of the present donor acceptor pairs (Table 2).

In nonpolar solvent NH, the rate constants of the present D−A pairs are of the same order of magnitude as those found in ACN. The values are presented in Table 2.

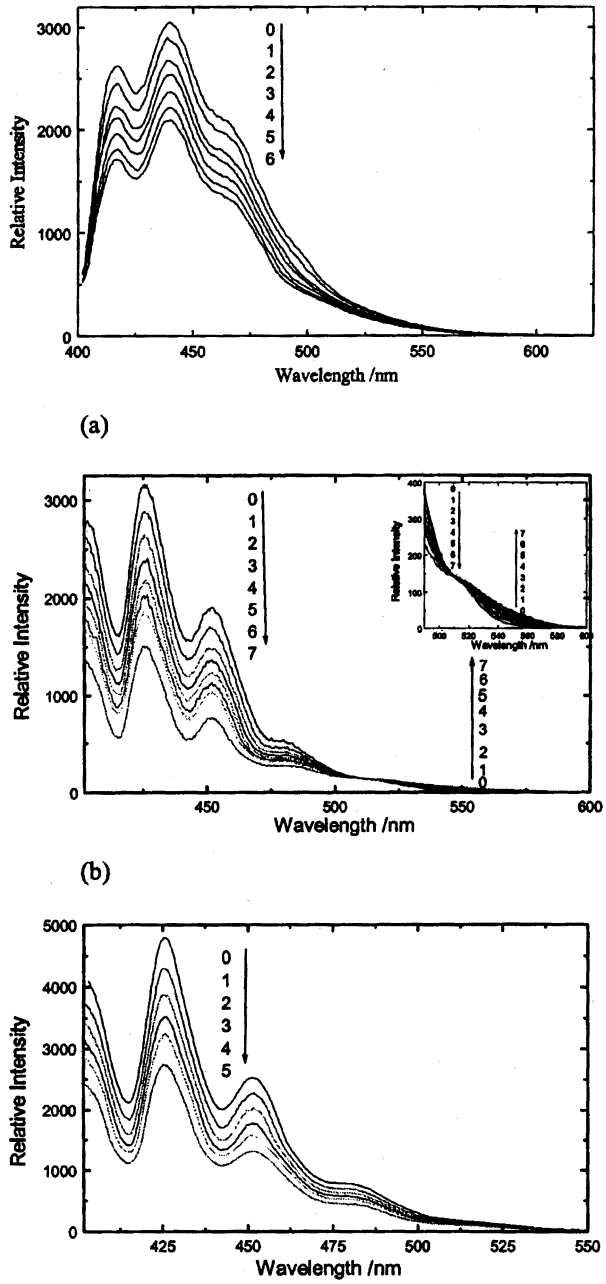

Figure 5. (a) Fluorescence emission spectra of 9CNA in ACN (concentration $\sim 1.8 \times 10^{-5}$ mol dm^{-3}) in the presence of 23DMI of concentration (mol dm^{-3}) in (0) 0, (1) 7.9×10^{-4}, (2) 1.6×10^{-3}, (3) 2.3×10^{-3}, (4) 3.1×10^{-3}, (5) 3.8×10^{-3}, and (6) 4.5×10^{-3}. (b) Fluorescence emission spectra of 9CNA in NH (concentration $\sim 2.0 \times 10^{-5}$ mol dm^{-3}) in the presence of 12DMI of concentration (mol dm^{-3}) in (0) 0, (1) 8.3×10^{-4}, (2) 1.7×10^{-3}, (3) 2.5×10^{-3}, (4) 3.3×10^{-3}, (5) 4.0×10^{-3}, (6) 4.8×10^{-3}, and (7) 6.7×10^{-3}. (c) Fluorescence emission spectra of 9CNA in NH (concentration $\sim 1.1 \times 10^{-5}$ mol dm^{-3}) in the presence of 23DMI of concentration (mol dm^{-3}) in (0) 0, (1) 7.9×10^{-4}, (2) 1.6×10^{-3}, (3) 2.4×10^{-3}, (4) 3.1×10^{-3}, and (5) 3.8×10^{-3}.

However in NH, in the presence of 12DMI (*N*-methyl substituted indole) the quenching phenomenon observed in 9CNA fluorescence was somewhat different (Figure 5b). When 9CNA fluorescence is quenched by 12DMI, a weak broad fluorescence band at around 520 nm appears at high quencher concentration (Inset of Figure 5b). Following the observations made by the earlier authors,[21] this band could be logically ascribed to an exciplex emission. Figure 5b shows a typical example where the isoemissive point is clearly observed. On the other hand, in the case of quenching by N−H indoles (23DMI, 25DMI), regular decrement in the entire 9CNA fluorescence band is observed (Figure 5c).

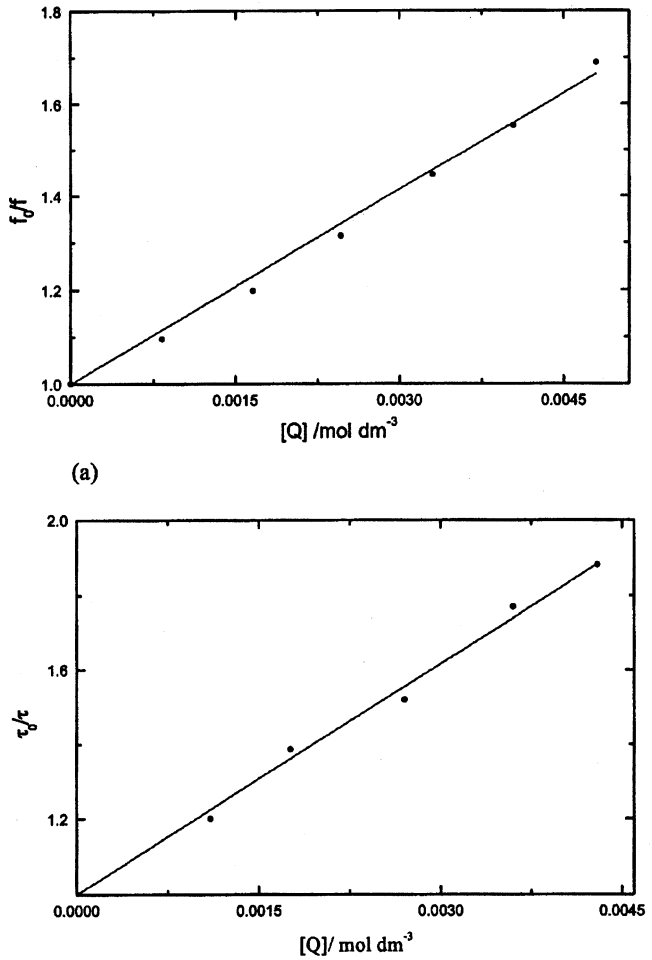

Figure 6. (a) Stern−Volmer (SV) plot from steady-state fluorescence emission intensity measurements in the case of singlet (S_1) excitation of 9CNA in the presence of 12DMI in NH fluid solution at 296 K. (b) Stern−Volmer (SV) plot from fluorescence lifetime measurements (time-resolved) in the case of singlet (S_1) excitation of 9CNA in the presence of 12DMI in NH fluid solution at 296 K.

It is well-known that polycyclic aromatic hydrocarbons and their derivatives form emissive exciplexes with electron donors in nonpolar solvents.[22] For indole and its derivatives, the only reported exciplex is for the quenching of pyrene and 9cyanopyrene by 12DMI.[21] In the studies of pyrene quenching by indole in solvents of varying polarity, exciplex emission was not observed.[23,24] Thus *N*-methyl substituted indoles are better candidates, relative to NH indoles, for the formation of emissive exciplex. The above-mentioned earlier observations are similar to the findings obtained with the present electron donor systems. In the present investigation, only 12DMI out of the three disubstituted indoles was observed to form emissive exciplex with 9CNA in nonpolar medium NH.

3.2.3. Transient Absorption Measurements. In laser flash photolysis experiments, pulsed laser excitation at 355 nm, using the third harmonic of a Nd:YAG laser was used to excite specifically the acceptor 9CNA molecule from the mixture of this acceptor and the donor 23DMI in both ACN and NH solvents. In this way, the possibility of concurrent occurrence of energy transfer (singlet−singlet) could be ignored as the first excited state (S_1) of the acceptor 9CNA lies below the corresponding level of the donor DMI molecule.

TABLE 2: Fluorescence Quenching Data for the Present D−A Systems at 296 K[a]

system	τ_0/ns (±0.4)	K_q/ dm^3 mol^{-1} s^{-1} × 10^{10}	K_d/ dm^3 mol^{-1} s^{-1} × 10^{10}
23DMI+9CNA*+ACN	16.1	2.08(2.18)	∼1.90
23DMI+9CNA*+EtOH	13.5	0.66(1.38)	∼0.61
23DMI+9CNA*+NH	15.6	1.37(2.05)	∼1.70
12DMI+9CNA*+ACN	16.1	0.84(1.46)	∼1.90
12DMI+9CNA*+EtOH	13.5	0.91(1.13)	∼0.61
12DMI+9CNA*+NH	15.6	1.17(1.50)	∼1.70
25DMI+9CNA*+ACN	16.1	1.50(1.70)	∼1.90
25DMI+9CNA*+EtOH	13.5	1.40(1.24)	∼0.61
25DMI+9CNA*+NH	2.5 DMI is sparingly soluble in NH		

[a] τ_0 denotes the acceptor fluorescence lifetime in the absence of the quencher, * denotes the excited singlet state. The values of k_q in parentheses are determined from the time-resolved spectroscopic technique, and the values outside the parentheses are measured from steady-state fluorescence methods.

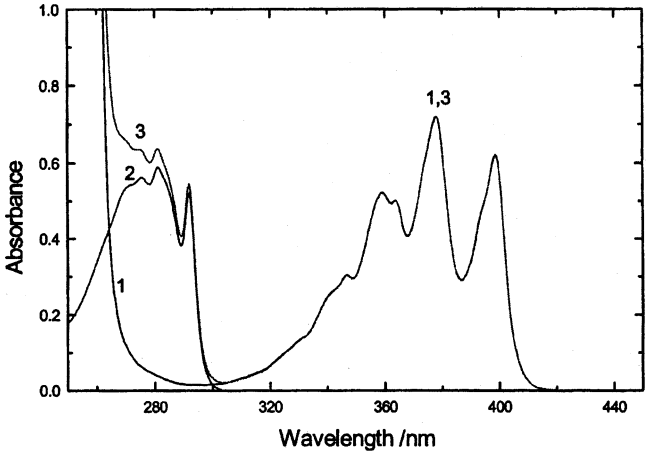

Figure 7. Steady-state electronic absorption spectra of (1) 9CNA (concentration ∼ 9.7 × 10^{-5} mol dm^{-3}), (2) 12DMI (concentration ∼ 1.23 × 10^{-4} mol dm^{-3}), and (3) the mixture of 9CNA and 12DMI in NH fluid solution at 296 K.

By using the laser flash photolysis technique, the transient absorption spectra of 9CNA was measured in the presence of 23DMI in both ACN and NH solvents. The spectra are shown in Figure 8. According to the earlier report[25,26] the broad spectrum observed around 560 nm in both of the solvents could be assigned to the band of 9CNA radical anion (9CNA$^-$) of the contact ion-pair. The decay at 560 nm corresponds very well to the first-order fitting. This corroborates our presumption of the formation of contact ion-pair (CIP) because the back charge transfer (charge recombination) within the contact ion-pairs obeys the first-order decay kinetics.

The time profile of the absorption of the acceptor 9CNA anion in ACN at 560 nm is reproduced in Figure 9. This absorption profile shows that, with further increase of the delay beyond 150 μs, the value of absorbance of the anion remains the same. When the constant absorbance value observed at long delay times is subtracted from the decay curve, the absorbance decay is represented approximately by a single exponential (shown in the inset of Figure 9) with a lifetime, τ_{ip}, (∼44.8 μs). The lifetime, τ_{ip}, is the ion-pair lifetime defined as in eqs 3 and 4

$$\tau_{ip} = (k_{cr} + k_{dis})^{-1} \quad (3)$$

$$\phi_R = k_{dis}\tau_{ip} \quad (4)$$

where k_{cr} and k_{dis} represent the rates associated with the geminate recombination and charge dissociation (solvent separated ion-pair formation) processes, respectively.

The yield ϕ_R of dissociated ion radical formations is obtained by taking the ratio of the constant absorbance at long delay

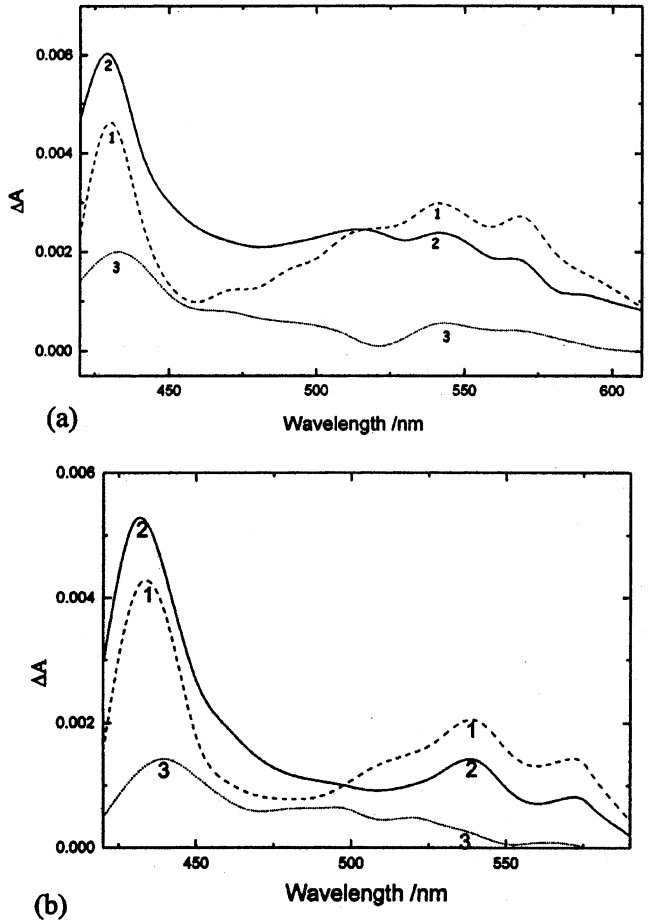

Figure 8. Transient absorption spectra of the mixture of 9CNA and 23DMI (excitation wavelength ∼355 nm, laser pulse energy ∼6 mJ pulse^{-1}) at the ambient temperature at delay times: (1) 10 μs, (2) 20 μs, and (3) 120 μs measured in (a) ACN and (b) NH.

times due to dissociated ions and the initial value estimated by extrapolating the ion absorbance to $t = 0$ in Figure 9. A low yield of the dissociated ion radical ($\phi_R \sim 0.15$) was obtained. The rates due to geminate ion-pair recombination (k_{cr}) and solvent separated ion-pair formation (k_{dis}) are computed using eqs 3 and 4 which are found to be nearly 1.9 × 10^4 and 3.3 × 10^3s^{-1} respectively for the present D−A system.

Following the earlier report,[27,28] the transient absorption band observed in both ACN and NH near 540 nm (Figure 8) could be assigned to the neutral radical of 23DMI (Scheme 1). It could be presumed that these neutral radicals are formed due to cleavage of N−H bond in GIP followed by H-abstraction (Scheme 1).

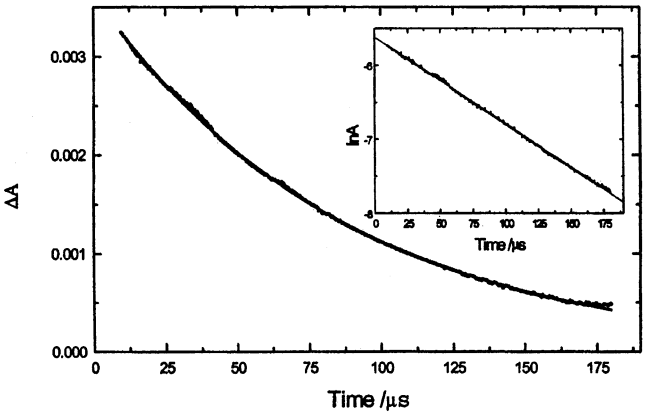

Figure 9. Time profile of the absorbance (A) of the acceptor 9CNA radical anion in the presence of 23DMI at 560 nm. Inset: Plot of ln *A* as a function of delay times, obtained by subtracting the constant value of absorbance at long delay time (>150 μs) from the observed decay curve.

SCHEME 1

CaseI: (In case of >N-H indole)

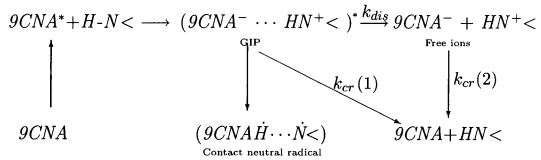

CaseII: (In case of N-substituted indole)

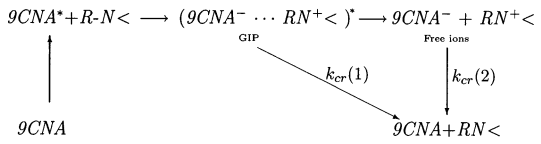

GIP: Geminate ion-pair

R = CH_3

* denotes excited singlet or triplet state

$k_{cr}(1)$ and $k_{cr}(2)$ represent the two different (1st and 2nd order) charge recombination processes

On looking to the transient absorption spectra of the mixture of the acceptor and 23DMI donor in both solvents (ACN and NH) (Figure 8a,b), one could see that with the increase of the delay times from 10 to 20 to 120 μs the anionic band at 560 nm decreases following the geminate charge recombination process. However, the time dependent behavior of the 430 nm band is different. With a gradual increase of delay (starting from 10 μs), the 430 nm band was found to be enhanced. It is noteworthy that the rise in absorbance at the 430 nm band is accompanied by the reduction of the absorption band at 560 nm. It appears that the building up of the monomer triplet of the acceptor 9CNA occurs at the same time interval during which the radical anionic species of it disappears. This demonstrates that the production of the monomeric triplet of 9CNA occurs through an ion recombination mechanism. In favor of the argument of formation of a monomer triplet of 9CNA, it could be stated that the measurements of kinetics of the absorption decay of the mixture at 430 nm were carried out and the decay was found to be single exponential in nature with the lifetime on the order of μs (in ACN, $\tau \approx 72$ μs and in NH, $\tau \approx 37$ μs). From the decay analysis, it is observed that the triplet lifetimes are much less than the lifetimes of the unperturbed triplet of 9CNA in the case of both solvents ACN and NH. It is to be mentioned that the lifetimes of the pure triplet of 9CNA are found to be on the order of 560 and 1700 μs in polar ACN and nonpolar NH solvents, respectively.[29,30] From the above observation of the formation of the locally excited triplet state of 9CNA from charge recombination, it appears that the process is exergonic; that is, the free energy of the triplet state of 9CNA is less than the free energy of the ion-pair. Thus, it is unlikely that the triplet state, after forming by the charge recombination process, would be involved with intermolecular ET (to form the ion-pair). As a plausible interpretation, it could be presumed that in this case conventional triplet−triplet (T−T) annihilation might occur in ACN at the delay times used when the transient triplet population is relatively large and the triplet quenching results.

SCHEME 2

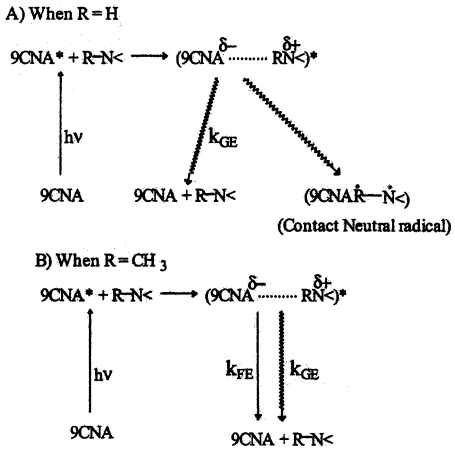

The transient absorption spectra of 9CNA in ACN or in NH in the presence of 12DMI do not show any band around the 540 nm regime where the neutral radical absorbs as discussed above. This is in accord with our expectation because, in the case of the N-substituted indoles, there is no possibility of formation of the neutral radical because of a lack of a H atom in the amino group unlike the cases of 23- and 25DMIs.

From all of the present observations, we can conclude that the photoinduced electron transfer is involved in the singlet quenching reactions. On the basis of the experimental results observed in the present study in ACN, Scheme 1 has been proposed.

Though the $k_{cr}(2)$ process has a possibility to occur in highly polar solvent ACN, from the present flash photolysis studies, such a process could not be detected.

In NH medium, the quenching mechanism appears to be entirely different. The quenching phenomenon (Figure 5b, Scheme 2) in this solvent is accompanied by the formation of an emissive exciplex (partial charge transfer) of type $(9CNA^{\delta-}....R-N^{\delta+}<)^*$. The rates of bimolecular quenching are observed to be nearly equal ($\sim 1.5 \times 10^{10}$ dm^3 mol^{-1} s^{-1}) for all of the present donors 23DMI, 12DMI, and 25DMI.

In Scheme 2, following Birks[31] nomenclature, k_{FE} and k_{GE} are the radiative and nonradiative rate constants for the exciplex decay. When R = CH_3, these are the only deactivation routes. However, for R = H, a new proton-transfer process offers an additional decay route for the exciplex.

Therefore, it is apparent that the decay of the exciplex depends strongly on the substitution on the N atom of the indole ring. When it is methyl substituted, exciplex emission is observed.

This emission is absent for N−H indoles. This behavior can be explained by a H-atom transfer reaction as an additional route for the fast decay of the exciplex formed in the nonpolar environment.

4. Concluding Remarks

Because of lower oxidation potential values of DMIs relative to those of monomethyl substituted indole derivatives, the former molecules appear to be better electron donors. In nonpolar medium, the decay of the exciplex depends strongly on the substitution on the N atom of the indole ring. In the case of N methyl substituted indole 12DMI, formation of the exciplex is facilitated. For N−H indoles, the absence of the exciplex even in nonpolar environment indicates that in these cases the H-atom transfer reaction acts as an additional route for the fast nonradiative decay of the exciplex. In ACN, the major nonradiative pathway is due to photoinduced ET rather than the formation of exciplex.

Acknowledgment. The authors are grateful to Dr. S. Goswami of the Department of Inorganic Chemistry for electrochemical measurements. Thanks are also due to the Department of Organic Chemistry for helping in purification of the samples. We express our heartiest thanks to Prof. S. Basak, K. Giri of Saha Institute of Nuclear Physics, Kolkata, India, Dr. H. Pal, and Mr. S. Nath of Radiation Chemistry and Chemical Dynamics Division of Bhabha Atomic Research Center, Trombay, Mumbai for fluorescence lifetime measurements. The authors are thankful to Dr. D. K. Palit of Radiation Chemistry and Chemical Dynamics Division of Bhabha Atomic Research Center, Trombay, Mumbai for helping in the measurements of the transient absorption spectra by laser flash photolysis technique. T.B. and T.M. acknowledge the financial support provided by the Council of Scientific and Industrial Research (CSIR), New Delhi, India in the form of grants and fellowships.

References and Notes

(1) Greenfield, S. R.; Seihert, M.; Govindjee.; Wasielewski, M. R. *Chem. Phys.* **1995**, *210*, 279.

(2) Prasad, E.; Gopidas, K. R. *J. Am. Chem. Soc.* **2000**, *123*, 1159.

(3) Axup, A. W.; Albin, M.; Mayo, S. L.; Crutchley, R. J.; Gray, H. B. *J. Am. Chem. Soc.* **1988**, *110*, 435.

(4) Book, L. D.; Arnett, D. C.; Hu, H.; Scherer, N. F. *J. Phys. Chem. A* **1998**, *102*, 4350.

(5) Mackintosh, J. G.; Mount, A. R. *J. Chem. Soc., Faraday Trans.* **1994**, *90*, 1121.

(6) Mackintosh, J. G.; Redpath, C. R.; Jones, A. C.; Langridge-Smith, P. R. R.; Reed, D.; Mount, A. R. *J. Electroanal. Chem.* **1994**, *375*, 163.

(7) Jennings, P.; Jones, A. C.; Mount, A. R.; Thomson, A. D. *J. Chem. Soc., Faraday Trans.* **1997**, *93*, 3791.

(8) Sinha, S.; De, R.; Ganguly, T. *Spectrochim. Acta Part A* **1998**, *54*, 145.

(9) Bhattacharya, T.; Misra, T.; Maiti, M.; Saini, R. D.; Chanda, M.; Lahiri, S.; Ganguly, T. *Spectrochim. Acta Part A* **2003**, *59*, 525.

(10) Ganguly, T.; Farmer, L.; Gravel, D.; Durocher, G. *J. Photochem. Photobiol. A: Chem.* **1991**, *60*, 63. Ganguly, T.; Farmer, L.; Li, W.; Bergeron, J. Y.; Gravel, D.; Durocher, G. *Macromolecules* **1993**, *26*, 2315.

(11) Sinha, S.; De, R.; Ganguly, T. *J. Phys. Chem. A* **1997**, *101*, 2852.

(12) Meech, S. R.; Phillips, D.; Lee, A. G. *Chem. Phys.* **1983**, *80*, 317.

(13) Jaffe, H. H.; Orchin, M. *Theory and application of ultraviolet spectroscopy*; John Wiley and Sons, Inc.: New York, 1962.

(14) Ganguly, T.; Farmer, L.; Gravel, D.; Durocher, G. *J. Photochem. Photobiol. A: Chem.* **1991**, *60*, 63.

(15) Sinha, S.; Ganguly, T. *J. Lumin.* **1998**, *79*, 201.

(16) Lakowicz, J. R. *Principles of Fluorescence Spectroscopy*; Plenum Press: New York, 1983; pp 127.

(17) Misra, T.; Ganguly, T.; Kamila, S.; Basu, C.; De, A. *Spectrochim. Acta Part A* **2001**, *57*, 2795.

(18) Rehm, D.; Weller, A. *Isr. J. Chem.* **1970**, *8*, 259.

(19) Rehm, D.; Weller, A. *Ber. Bunsen-Ges. Phys. Chem.* **1969**, *73*, 837.

(20) Kikuchi, K. *J. Photochem. Photobiol. A: Chem.* **1992**, *65*, 149.

(21) Eriksen, J.; Foote, C. S. *J. Phys. Chem.* **1978**, *82*, 2659.

(22) Palmas, J. P.; Vander Auweraer, M.; Swinnen, A. M.; De Schryver, F. C. *J. Phys. Chem.* **1984**, *106*, 7721.

(23) Montejano, H. A.; Cosa, J. J.; Garrera, H. A.; Previtali, C. M. *J. Photochem. Photobiol. A: Chem.* **1995**, *86*, 115.

(24) Borsarelli, C. D.; Montejano, H. A.; Cosa, J. J.; Previtali, C. M. *J. Photochem. Photobiol. A: Chem.* **1995**, *91*, 13.

(25) Manring, L. E.; Gu, Chee-Hang; Foote, C. S. *J. Phys. Chem.* **1983**, *87*, 40.

(26) Zimmermann, C.; Mohr, M.; Zipse, H.; Eichherger, R.; Schnabel, W. *J. Photochem. Photobiol. A: Chem.* **1999**, *125*, 47.

(27) Zhang, X.; Erb, C.; Flammer, J.; Nau, W. M. *Photochem. Photobiol.* **2000**, *71*, 524.

(28) Shida, T. *Electronic Absorption Spectra of Radical ions*; Elsevier: Amsterdam, 1988.

(29) Vanderdonckt, E.; Barthels, M. R.; Delstinne, A. *J. Photochem.* **1973**, *1*, 429.

(30) Maiti, M.; Misra, T.; Sinha, S.; Pal, S. K.; Mukherjee, D.; Saini, R. D.; Ganguly, T. *J. Lumin.* **2001**, *93*, 261.

(31) Birks, J. B. *Photophysics of Aromatic Molecules*; Wiley: London, 1970.